Inorganic Chemistry

Article

pubs.acs.org/IC

Modeling Biological Copper Clusters: Synthesis of a Tricopper Complex, and Its Chloride- and Sulfide-Bridged Congeners

Gianna N. Di Francesco, Aleth Gaillard, Ion Ghiviriga, Khalil A. Abboud, and Leslie J. Murray*

Department of Chemistry, Center for Catalysis, University of Florida, Gainesville, Florida 32611-7200, United States

Supporting Information

ABSTRACT: The synthesis and characterization of a family of tricopper clusters housed within a tris(β-diketimine) cyclophane ligand (H_3**L**) that bear structural similarities to biological copper clusters are reported. In all complexes, each Cu atom is held within the N_2-chelate of a single β-diketiminate arm. Reaction of $\mathbf{L}^{3-}$ with CuCl affords an anionic complex containing a μ_3-chloride donor in the central cavity, whereas there is no evidence for bromide incorporation in the product of the reaction of $\mathbf{L}^{3-}$ with CuBr (Cu_3**L**). Cu_3**L** reacts with elemental sulfur to generate the corresponding air-stable mixed-valent (μ_3-sulfido)tricopper complex, $Cu_3(\mu_3\text{-}S)$**L**, which represents the first example of a sulfide-bridged copper cluster in which each metal center is both coordinatively unsaturated and held within a N-rich environment. The calculated LUMO is predominantly Cu−S π* in character and delocalized over all three metal centers, which is consistent with the isotropic ten-line absorption ($g \sim 2.095$, $A \sim 33$ G) observed at room temperature in EPR spectra of the one-electron chemically reduced complex, $[Cu_3(\mu_3\text{-}S)\mathbf{L}]^-$.

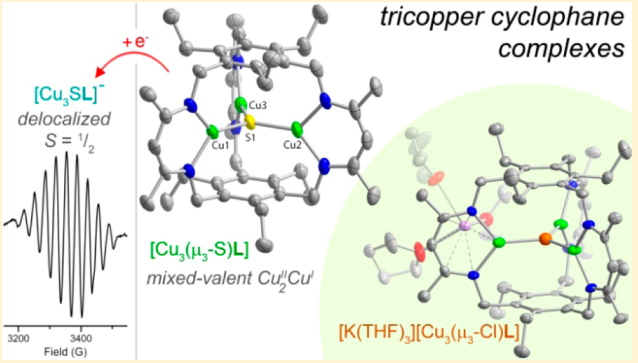

INTRODUCTION

The diverse functions of multicopper clusters in biological systems, such as methane hydroxylation,[1] ion-transport and substrate oxidation,[2] and nitrous oxide reduction,[3] suggest that the similar reactivity can be accessed in polynuclear synthetic complexes. Model clusters of the tricopper cluster in MCOs have been synthesized by reaction of mononuclear complexes with dioxygen; however, this synthetic approach typically generates di(μ_3-oxo)tricopper cores for which the O···O vector lies perpendicular to the tricopper plane,[4] which contrasts the proposed coplanar orientation of the O_2-fragment with the three metal centers in the enzyme active site.[2] To access MCO-like intermediates, we sought to develop tricopper complexes in which ligand steric effects enforce the orientation of dioxygen binding. Here, we report the synthesis of a coordinatively unsaturated tricopper(I) cluster, Cu_3**L** (**1**), wherein the cyclophane ligand can accommodate only one μ_3-donor as observed in the chloride-bridged analogue, $[Cu_3(\mu_3\text{-}Cl)\mathbf{L}]^-$ (**2**).

The Cu_Z cluster in N_2OR has been reported with two compositions depending on the method used for protein isolation for crystallization: a $Cu_4(\mu_2\text{-}S)(\mu_4\text{-}S)$ cluster, termed CuZ, and a $Cu_4(\mu_4\text{-}S)$, or CuZ*.[3b−e] Model complexes that incorporate either $Cu_n(\mu_n\text{-}S)$ or $Cu_n(\mu_n\text{-}S)(\mu_2\text{-}S)$ motifs in which the copper ions are coordinatively unsaturated and held in a nitrogen-rich donor set can provide invaluable insight into the reaction mechanisms of N_2O activation by reduced CuZ and CuZ*. However, synthetic clusters of these types have been elusive. Previously, reaction of mononuclear copper(I) compounds with S-atom sources (e.g., S_8 or Na_2S_2) afforded di- and tricopper complexes bridged by disulfide or subsulfide, and S-atom transfer reagents have led to higher nuclearity clusters with two S-atom bridges.[5] In addition to **1** and **2**, we also report the facile and selective synthesis of a coordinatively unsaturated, mixed-valent (μ_3-sulfido)tricopper(II/II/I) cyclophane complex **3**, and its chemical reduction to an anionic $Cu_2^ICu^{II}$ species, **4**.

EXPERIMENTAL METHODS

General Considerations. All reactions were performed under a dinitrogen atmosphere in an Innovative Technologies glovebox. Solvents were purchased from Sigma-Aldrich, then dried using an Innovative Technologies solvent purification system, and stored over activated 3 Å molecular sieves. Reagents were purchased from Sigma-Aldrich or Strem Chemicals and used as received unless stated otherwise. Deuterated solvents were purchased from Cambridge Isotope Laboratories (CIL), purified according to reported procedures and then stored over activated 3 Å molecular sieves.[6] Isotopically-enriched sulfur (^{34}S) was purchased from CIL and dried under vacuum at room temperature overnight. Elemental sulfur was sublimed, recrystallized from benzene in the dark, and stored away from light.[7] CuBr was dried under vacuum at 175 °C overnight. Cp^*_2Co was sublimed at 20 mTorr and 215 °C, then recrystallized from hexanes, and stored at −35 °C. NMR spectra were collected on a Varian Inova operating at 500 MHz for ^{1}H, equipped with a three-channel 5 mm indirect detection probe with z-axis gradients. ^{13}C and ^{15}N chemical shifts were measured in gHMBC experiments. All chemical shifts are reported in parts per million (ppm), and referenced to tetramethylsi-

Received: February 11, 2014
Published: April 18, 2014

   dx.doi.org/10.1021/ic500333p | Inorg. Chem. 2014, 53, 4647−4654

lane for ^{1}H and ^{13}C, and to neat ammonia for ^{15}N. UV−visible−nIR absorption spectra were collected using a Varian Cary 50 spectrophotometer and quartz cuvettes having a 1 cm path length and air-free screw top seal (Starna Cells Inc., Atascadero, CA, USA). For low-temperature UV−visible−nIR measurements, the spectrophotometer was fitted with an evacuated, helium-cooled cyrostat equipped with an Air Products and Chemicals Inc. compressor 1R04WSL, expander module DE202, Au Chromel thermocouple, and a Scientific Instruments temperature controller 9600-5a.[8] IR spectra were collected in a nitrogen-filled glovebox using a Bruker Alpha with an ATR diamond crystal stage using the Opus 7.0 software package. Far-IR spectra were collected using a Bruker Vertex 80v with a Bruker Hg lamp source and a Pike GladiATR ATR stage purged with nitrogen gas using Opus 6.5 software. Electrospray mass spectra were collected by direct injection into an Aglient 6120 TOF spectrometer at a gas temperature of 100 °C and fragmentation voltage of 120 V on solution samples prepared in a nitrogen atmosphere glovebox and transported in Hamilton gastight sample-lock syringes. Cyclic voltammetry and differential pulse voltammetry experiments were performed in a nitrogen atmosphere glovebox using a Princeton Applied Research Versastat II potentiostat and a three-electrode setup (1 mm Pt button working, Pt wire counter, and Ag/Ag^{+} reference) with electrodes purchased from BASi, Inc. and/or CH Instruments, Inc. EPR measurements were recorded on a Bruker Elexsys E580 with a Bruker 4116DM resonator. Data were collected in the field from 50 to 7050 G with the following parameters for (298 K): power = 2.002 mW; frequency = 9.809 GHz; modulation frequency = 100.00 kHz; modulation amplitude = 5 G; and gain = 70 dB; and for (5−90 K): power = 6.30 × 10^{-2} mW; frequency = 9.622 GHz; modulation frequency = 100.00 kHz; modulation amplitude = 10.00 G; and gain = 60 dB. Complete Analysis Laboratories, Inc. (Parsippany, NJ) conducted elemental analyses on samples shipped under an inert atmosphere. The ligand, H_3**L**, was synthesized as described previously.[9]

X-ray Crystallography. *[Cu_3ClL]*$^{-}$. X-ray intensity data were collected at 100 K on a Bruker DUO diffractometer using Mo Kα radiation (λ = 0.71073 Å) and an APEXII CCD area detector. Raw data frames were read by the SAINT program[28] and integrated using 3D profiling algorithms. The resulting data were reduced to produce *hkl* reflections and their intensities and estimated standard deviations. The data were corrected for Lorentz and polarization effects, and numerical absorption corrections were applied based on indexed and measured faces. The structure was solved and refined in SHELXTL6.1,[29] using full-matrix least-squares refinement. The non-H atoms were refined with anisotropic thermal parameters, and all of the H atoms were calculated in idealized positions and refined riding on their parent atoms. The unit cell consists of the Cu3 complex anion, a potassium cation, and four THF solvent molecules. Only one of the THF molecules is not coordinated to the potassium cation. In the final cycle of refinement, 13 553 reflections (of which 11 381 are observed with $I > 2\sigma(I)$) were used to refine 691 parameters and the resulting R_1, wR_2, and S (goodness of fit) were 3.00%, 6.20%, and 0.971, respectively. The refinement was carried out by minimizing the wR_2 function using F^2 rather than F values. R_1 is calculated to provide a reference to the conventional R value, but its function is not minimized.

Cu_3SL. X-ray intensity data were collected at 100 K on a Bruker DUO diffractometer using Cu Kα radiation (λ = 1.54178 Å), from an ImuS power source, and an APEXII CCD area detector. Raw data frames were read by the SAINT program and integrated using 3D profiling algorithms. The resulting data were reduced to produce *hkl* reflections and their intensities and estimated standard deviations. The data were corrected for Lorentz and polarization effects, and numerical absorption corrections were applied based on indexed and measured faces. The structure was solved and refined in SHELXTL6.1, using full-matrix least-squares refinement. The non-H atoms were refined with anisotropic thermal parameters, and all of the H atoms were calculated in idealized positions and refined riding on their parent atoms.

Density Functional Theory Calculations. Geometry optimizations were first conducted with Gaussian 09 using density functional theory (DFT) at the B3YLP level of theory. C, H, and N atoms were calculated using the basis set 6-31G(d), S using 6-31+G(d), and Cu using LANL2DZ, and then repeated as before with the only change being that the LANL2DZ basis set was used instead for S.[10] The crystallographic coordinates were used as the starting point for all geometry optimizations. Single-point calculations were performed on the crystallographic coordinates using LANL2DZ ECP on all atoms.

Cu_3L (1). H_3**L** (300 mg, 0.434 mmol) and benzyl potassium[11] (178 mg, 1.37 mmol) were dissolved in THF (15 mL) at −90 °C and allowed to warm to room temperature and stirred for 30 min. Approximately 15 mL of the solvent were then removed in vacuo from the purple reaction mixture, toluene (15 mL) was added, and the reaction cooled to −35 °C. A slurry of CuBr (189 mg, 1.32 mmol) in cold toluene (3 mL) was added dropwise to the solution of the deprotonated ligand, which was stirred overnight at −35 °C. The reddish-brown reaction mixture was then filtered through 0.2 μm nylon filter paper and then through toluene-rinsed Celite. The solvent was removed from the red filtrate under reduced pressure to afford a dark red powder (39%). Elemental analysis for $C_{45}H_{63}N_6Cu_3$: % Calculated C, 61.51; H, 7.23; N, 9.56; Cu, 21.70; % Found C, 62.17; H, 7.11; N, 9.59; Cu, 21.58. IR (cm^{-1}): 1518, 1396, 1325, 1014. ^{1}H NMR (299 MHz, C_6D_6) δ (ppm): 1.16 (t, J = 7.31 Hz, 18 H), 2.09 (s, 18 H), 2.64 (q, J = 7.31 Hz, 12 H), 4.56 (s, 12 H), 4.85 (s, 3 H). ^{13}C NMR (500 MHz, C_6D_6) δ (ppm): 16.8, 22.7. 23.0, 49.4, 95.9, 138.0, 144.1, 164.9. ^{15}N NMR (500 MHz, C_6D_6) δ (ppm): 201.1.

[K(THF)$_3$][Cu_3ClL] (2). H_3**L** (300 mg, 0.434 mmol) and benzyl potassium[11] (178 mg, 1.37 mmol) were dissolved in THF (15 mL) at −90 °C and allowed to warm to room temperature and stirred for 30 min. A slurry of CuCl (130 mg, 1.32 mmol) in cold THF (3 mL) was added dropwise to the reaction mixture, which was allowed to stir overnight at −35 °C. The orange-tan reaction mixture was then filtered through 0.2 μm nylon filter paper and then through THF-rinsed Celite. The solvent was removed under reduced pressure from the orange-tan filtrate to afford a dark yellow powder (48%). Yellow crystals were grown via a diffusion of pentane into a THF solution of **2**. Elemental analysis for $C_{57}H_{87}N_6O_3Cu_3ClK$: % Calculated C, 59.05; H, 7.05; N, 8.83; % Found C, 59.04; H, 7.03; N, 9.07. ^{1}H NMR (299 MHz, d_8-THF) δ (ppm): 1.08 (t,18 H), 1.94 (s, 18 H) 2.45 (q, 12 H), 4.21 (s, 3 H), 4.36 (s, 12 H). HRMS (ESI-TOF) m/z: [Cu_3Cl**L**]$^{-}$ Calcd, 913.2682 for $C_{45}H_{63}Cu_3N_6Cl$; Found, 913.2650.

Cu_3SL (3). A solution of S_8 (22 mg, 0.086 mmol) in THF (3 mL) was added dropwise to a stirred solution of Cu_3**L** (300 mg, 0.343 mmol) in THF (15 mL) at −35 °C. The reaction mixture was allowed to stir overnight at −35 °C and then filtered first through a fine-porosity glass frit and then through THF-rinsed Celite. The resulting green filtrate was dried in vacuo to give the product as a dark green powder (33%). Dark green crystals were grown via a slow evaporation of a benzene solution of **3** into *m*-xylenes. Elemental analysis for $C_{45}H_{63}N_6Cu_3S$: % Calculated C, 59.35; H, 6.97; N, 9.23; S, 3.52; Cu, 20.93; % Found C, 59.12; H, 7.09; N, 8.88; S, 3.32; Cu, 21.22. IR (cm^{-1}): 1528, 1400, 1331, 1012. ^{1}H NMR (299 MHz, C_6D_6) δ (ppm): 1.17 (t, J = 7.49 Hz, 18 H), 2.05 (s, 18 H), 2.74 (q, J = 7.55 Hz, 12 H), 4.41 (s, 12 H), 4.93 (s, 3 H). ^{13}C (500 MHz, C_6D_6) δ (ppm): 16.3, 22.6, 22.8, 50.8, 97.6, 137.2, 144.1, 164.2. ^{15}N (500 MHz, C_6D_6) δ (ppm): 181.3. HRMS (ESI-TOF) m/z: [M + H]$^{+}$ Calcd 911.2784 for $C_{45}H_{63}Cu_3N_6{}^{32}S$, Found 911.2791; Calcd 913.2784 for $C_{45}H_{63}Cu_3N_6{}^{34}S$, Found 913.2739.

Chemical Reduction of 3 with Cp*$_2$Co. A portion of Cu_3SL (20 mg, 0.02 mmol) was dissolved in THF (∼10 mL) and cooled to −35 °C. A solution of Cp*$_2$Co (7 mg, 0.02 mmol) in THF (4 mL) at −35 °C was then added dropwise to the reaction mixture, which was allowed to stir overnight at −35 °C. The reaction was filtered through a fine porosity frit and then again through THF-rinsed Celite. Solvent was removed from the filtrate in vacuo to yield an aqua powder (84%). Elemental analysis for $C_{65}H_{93}N_6Cu_3Co$: % Calculated C, 62.95; H, 7.56; N, 6.78; % Found C, 63.23; H, 7.88; N, 6.92. HRMS (ESI-TOF) m/z: [Cu_3S**L**]$^{-}$ Calcd 910.2706 for $C_{45}H_{63}Cu_3N_6S$; Found 910.2706.

Reaction of 1 with Me$_3$PS. A portion (10 mg, 0.01 mmol) of Cu_3**L** was dissolved in THF (∼5 mL), and the solution was cooled to −35 °C. A solution of Me_3PS (1 mg, 0.01 mmol) in THF (∼2 mL)

dx.doi.org/10.1021/ic500333p | Inorg. Chem. 2014, 53, 4647−4654

Scheme 1. Synthesis of Tricopper Complexes

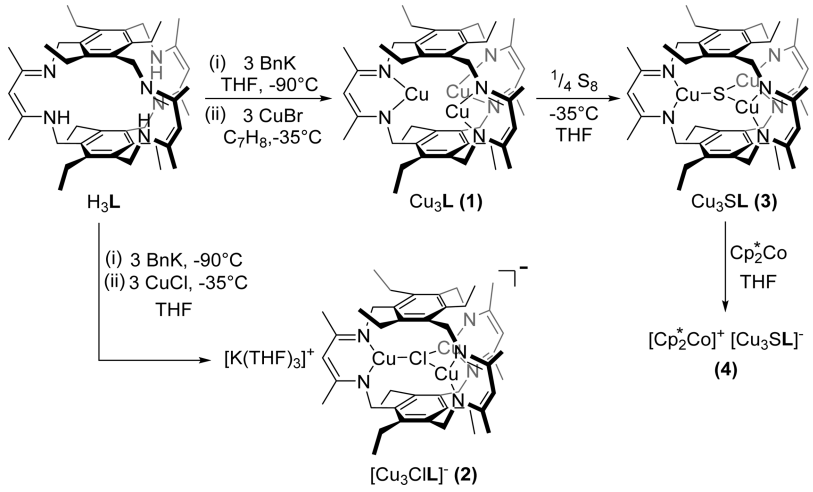

was added dropwise to the stirring cold reaction mixture. The reaction was allowed to stir at −35 °C overnight to afford a pale orange reaction mixture, which was filtered through a 0.2 μm nylon filter paper and then THF-rinsed Celite. The resulting filtrate was dried in vacuo, and the ^{1}H NMR spectrum of the residue was recorded in d_6-benzene.

Reaction of 1 with PMe_3. To a room-temperature solution of Cu_3**L** (15 mg, 0.02 mmol) in toluene (∼5 mL) was added either 1.01 or 3.03 equiv of PMe_3 (17 and 52 μL, 1 M solution in toluene) with vigorous stirring. Addition of phosphine resulted in an immediate color change for both reactions, with the higher equivalents of PMe affording a pale yellow mixture versus the pale orange reaction mixture for the reaction with 1.01 equiv. The mixtures were allowed to stir at room temperature for ∼30 min, after which the volatiles were removed under reduced pressure and ^{1}H NMR spectra were collected on the residues in d_6-benzene.

Synthesis of 3 in the Presence of 9,10-Dihydroanthracene. Reaction procedure is as reported for Cu_3**SL** except that 10 equiv. 9,10-dihydroanthracene were included in the S_8 solution.

RESULTS

Syntheses and Molecular Structures of Cu_3L, $[Cu_3ClL]^-$, and Cu_3SL. As expected from our previous work with this ligand, reaction of the in situ generated potassium salt of L^{3-} with either copper bromide or chloride afforded the tricopper complexes Cu_3**L** (**1**) and $[Cu_3(\mu_3\text{-Cl})L]^-$ (**2**) as dark red and yellow-brown solids, respectively (Scheme 1). Both reactions, however, required low-temperature and portion-wise addition of the copper(I) precursor to the deprotonated ligand to limit Cu^0 formation. Disproportionation was unexpected as it was reported only for metalation of electron-deficient β-diketiminates with copper halides and likely contributes to the moderate yields of both **1** and **2**.[12]

We have been yet unable to obtain single crystals of **1** and, therefore, pursued multidimensional NMR to interrogate the structure in solution. HMBC spectra of Cu_3**L** indicate that the complex is D_{3h}-symmetric in solution on the NMR time scale, and the downfield shifts for the ^{14}N and ^{1}H resonances of the β-diketiminate (nacnac) N atoms and −C**H** protons, respectively, relative to the free ligand are consistent with copper(I) coordination (Figures S2 and S4, Supporting Information).[12,13] Low-temperature ^{1}H NMR spectra recorded in d_8-THF are also consistent with a D_{3h}-symmetric compound, implying uniform coordination environments around each copper center (Figure S5, Supporting Information).

In contrast to Cu_3**L**, pentane diffusion into a THF solution of **2** afforded single crystals of sufficient quality for X-ray diffraction experiments. In the molecular structure, each Cu^I center adopts a trigonal-planar coordination environment composed of two N-donors from one β-diketiminate arm and the chloride donor housed within the internal cavity of the cyclophane (Figure 1). The N−Cu−N bond angles are more

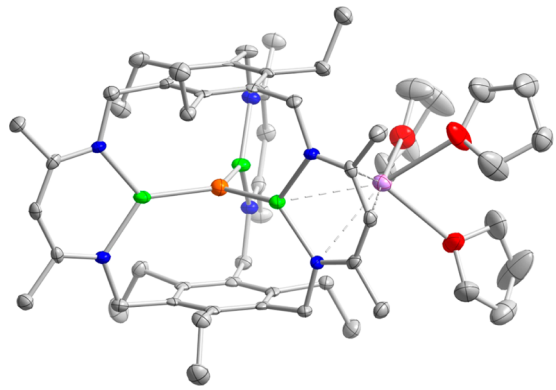

Figure 1. Molecular structure of **2** at 65% thermal ellipsoid. The chloride donor is housed within the central cavity, affording three-coordinate Cu(I) centers, and a potassium countercation is coordinated to one Cu(nacnac) arm. Gray, blue, red, green, lavender, and orange ellipsoids correspond to C, N, O, Cu, K, and Cl atoms, respectively. Hydrogen atoms have been omitted for clarity.

obtuse (103.3−105.3°) than those observed in the mononuclear copper−nacnac complexes, which could arise from the steric requirements to accommodate the μ_3-chloride donor or from differences between the steric repulsions within each nacnac arm (viz. N-atom substituents and the Me groups) as compared to other mononuclear species. Previously, we reported that bromide incorporation within the internal cavity was accompanied by ligand distortions (e.g., dihedral angle between the two aromatic rings);[9] however, the smaller halide is readily accommodated in **2**, leading to almost parallel aryl planes (1.9°). Consistent with our prediction for **1**, the $Cu^I\cdots Cu^I$ distances in **2** are similar to those reported for the tricopper cluster in MCOs.[5b,c] The potassium countercation coordinates to one of the Cu(nacnac) units, which is atypical for anionic transition-metal−nacnac complexes with alkali countercations.

dx.doi.org/10.1021/ic500333p | Inorg. Chem. 2014, 53, 4647−4654

As might be expected, the K−Cu(nacnac) are very comparable to those reported for K−arene interactions (3.129−3.744 Å).[14]

The comparable ionic radii of S^{2-} and Cl^- suggested that an analogous sulfide-bridged complex could be accessed.[15] Indeed, reaction of Cu_3**L** with elemental sulfur in THF yields a dark-green mixture from which the air-stable mixed-valent sulfide-bridged tricopper cluster, Cu_3S**L** (**3**), (33% yield) can be separated from an intractable precipitate. The expected $[M + H]^+$ ion for Cu_3S**L** is observed in ESI(+) mass spectra for solutions of **3** synthesized using natural abundance or isotopically -enriched $^{34}S_8$ (Figure S13, Supporting Information). Similar to **1** and **2**, 2-D NMR and variable-temperature ^{1}H NMR spectra suggest a D_{3h}-symmetric species in solution. The sharp resonances observed in these spectra support an $S = 0$ ground state for this complex, which is consistent with X-band EPR measurements (Figures S9 and S15, Supporting Information).

In the solid-state structure, Cu_3S**L** adopts pseudo-D_{3h} symmetry with near equivalent Cu−S−Cu angles and with the sulfide donor coplanar with the three copper ions. Minor differences are observed in the Cu−S distances, which vary from 2.1035 to 2.1085 Å (Figure 2 and Figure S16, Supporting Information). With respect to other synthetic copper clusters containing S atom bridges (viz. two bridging sulfides or a bridging disulfide) and N-donor ligands, the bonds between the copper and sulfur centers in **3** are shorter (0.076−0.138 Å), which likely arise from the steric constraints enforced by the cylcophane cavity.[5a−e,g] The copper−chalcogenide distances here are similar to those observed in the Cu_Z cluster forms, which range from 1.9−2.4 Å in CuZ and 2.2−2.3 Å in CuZ* for the copper ions coordinated by two His residues.[3d] The planar arrangement of three metal ions and the μ_4-sulfide, albeit trigonal in **3**, and the number of N-atom donors are comparable to the Cu_3S fragment of CuZ composed of Cu1, Cu2, and Cu3. Each Cu(nacnac) unit is structurally analogous to previously reported monometallic complexes, with similar N−Cu distances (1.9279−1.9355 Å) and slightly larger N−Cu−N angles (99.0−99.4°).[16] As compared to **2**, both the N−Cu and the N−Cu−N bond angles are shorter, and the former is consistent with the higher oxidation of the cluster in **3** (i.e., $Cu_2^{II}Cu^{I}$) as compared to the zero-hole (i.e., Cu_3^{I}) cluster in **2**. In the space-filling representation of **2**, it is clear that the S atom is in close contact with the two aromatic rings of the cyclophane with aryl centroid-to-sulfide distances of 2.9791 and 2.9725 Å, and these distances are the shortest crystallographically reported between a S atom and an aromatic π-system (Figure S16, Supporting Information).[17]

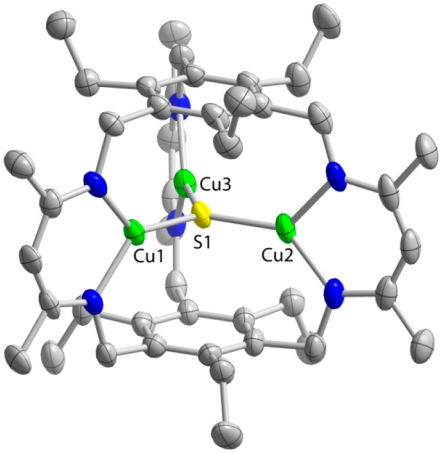

Figure 2. Molecular structure of **3** at 65% thermal ellipsoid. The mixed-valence complex contains an inorganic sulfide in close proximity to the centroid of both triethylbenzene units, and three coordinatively unsaturated copper centers. Gray, blue, green, and yellow ellipsoids correspond to C, N, Cu, and S atoms, respectively. Hydrogen atoms have been omitted for clarity.

Electrochemistry and Absorption Spectroscopy of 3. In cyclic voltammograms, we observe a reversible one-electron redox process assigned to the $[Cu_3S]^{3+/2+}$ couple at $E_{1/2}$ = −1.44 V versus Fc/Fc^+ and two irreversible oxidations at −0.93 and 0.01 V (Figure 3). Using differential pulse voltammetry, the reversible wave is confirmed to be a one-electron process as $\Delta\omega_{1/2} \approx 100$ mV (Figures S17 and S18, Supporting Information). The irreversible oxidation at 0.01 V likely results in complex degradation as suggested by the decrease in peak current for the reversible wave after repeated scans to potentials greater than 0.01 V. Concomitant with the loss in peak current for the wave at −1.44 V, we also observe an increase in the current at −0.93 V (data not shown). The width at half-height for the differential pulse voltammograms for the oxidation at 0.01 V is consistent with a one-electron oxidation; however, peaks at slightly higher potentials are significantly broader, which is expected for irreversible processes (Figure S17, Supporting Information). To estimate the extent of charge delocalization in **3**, the potentials for the two oxidative waves were used to calculate the lower limit for the comproportionation constant, K_c, and free energy, ΔG_c^0.[18] The large values determined for K_c and ΔG_c^0 of 3.12×10^{23} and −134 kJ/mol, respectively, support the assignment of this complex as a valence-delocalized class III cluster using the Robin−Day classification.

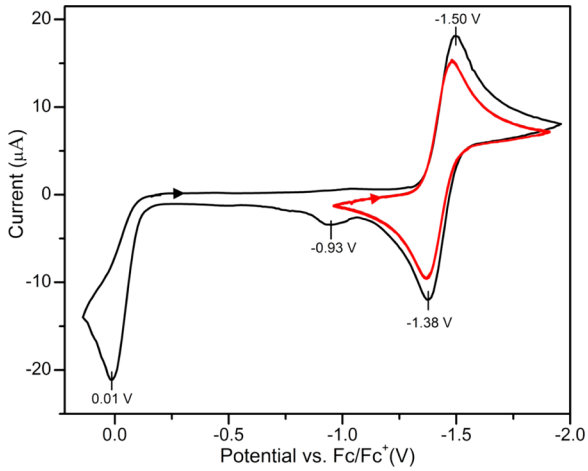

Figure 3. Cyclic voltammogram of $Cu_3(\mu_3\text{-S})$**L** in dichloromethane using 0.3 M $TBAPF_6$ as a supporting electrolyte and a scan rate of 100 mV/s. Working electrode: 1 mm Pt button; reference electrode: $Ag/AgNO_3$ in MeCN; auxiliary electrode: Pt wire.

Absorption maxima centered at 32 000 cm^{-1} (ε_{312} = 19 000 $M^{-1}cm^{-1}$) with a shoulder at 29 600 cm^{-1} (ε_{338} = 27 000 M^{-1} cm^{-1}), and 12 400 cm^{-1} (ε_{806} = 8700 M^{-1} cm^{-1}), are present in the UV−visible−nIR absorption spectra of solutions of Cu_3S**L** (Figure 4). This spectrum bears similarities with those reported previously for the self-assembled tricopper clusters, CuZ, and CuZ*, specifically one visible-to-nIR electronic absorption band

dx.doi.org/10.1021/ic500333p | Inorg. Chem. 2014, 53, 4647−4654

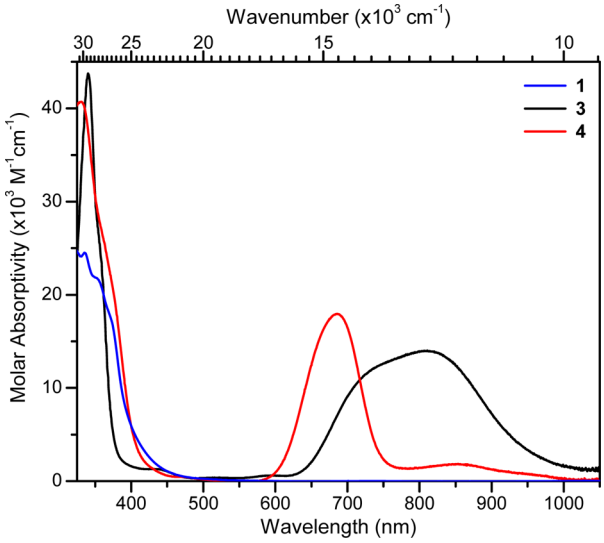

Figure 4. Extinction coefficient plot for **1** (blue line), **3** (black line), and **4** (red line) in tetrahydrofuran. For **1**, the near-UV absorption feature (λ_{max} = 323 nm) and the absence of other features in the visible region are comparable to other reported tri- and tetranuclear copper(I) complexes. Spectra for **3** and **4** with maxima at 806 and 686 nm are similar to those reported for chalcogenide-bridged mixed-valence clusters.

in the spectrum.[5g] In prior reports, this transition was centered at ~650 nm ($\varepsilon \sim 3500$ M^{-1} cm^{-1}) and attributed to an S(p) → Cu(3d) charge transfer, but we cannot rule out contributions from other ligand−metal charge transfers in **3**. The intervalence charge-transfer bands reported for a series of rigid trigonal-planar (μ_3-oxo)tricopper clusters are of comparable energy to the nIR feature observed in Cu_3**SL**.[19] However, the profile of the 806 nm feature for **3** lacks the asymmetry predicted for a class III valence-delocalized complex and is more consistent with a valence-trapped species.[20] In variable-temperature UV−visible−nIR spectra recorded on solutions of Cu_3**SL** in either 2-methyltetrahydrofuran or THF, the intensity of the nIR band increases until 248 K, below which only subtle changes to the peak shape are observed (Figure S21, Supporting Information). These results contradict the electrochemical analysis (vide supra) and the absence of a solvent dependence for the absorption spectrum (Figure S22, Supporting Information), suggesting that this complex may lie between Class II and III or that other factors (e.g., vibrational modes or low-lying excited states) may prevent a simple two-state treatment. In addition to UV−visible−nIR absorption spectra, we collected far-infrared spectra on solid samples of **3**. Two fIR absorptions are observed at 386 and 300 cm^{-1}, of which the 386 cm^{-1} peak shifts to 382 cm^{-1} in ^{34}S isotopically labeled samples (Figure S19, Supporting Information). These frequencies are comparable to those for Cu−S stretching modes in previously synthesized multicopper complexes containing S atom bridges and for those in the CuZ* cluster.[5g,21]

Density Functional Calculations on 3. To gain further insight into the electronic structure of the cluster, we performed single-point calculations on the crystallographic coordinates for complex **3**. Geometry optimizations on either the solid-state structure or a truncated complex (i.e., Me for Et substitution) afforded significantly longer Cu−S bonds (~2.161 Å), N−Cu−N bond angles (~102°), and arene−S distances (~3.029 Å) than those observed in the molecular structure. The HOMO to HOMO-6 differ by approximately 1 eV with the HOMO to HOMO-2 derived from nonbonding β-diketiminate π-orbitals, and the HOMO-3 and HOMO-4 arising from σ*-interactions between the Cu 3d$_{yz}$ and nacnac N atoms (Figure 5 and Figure S23, Supporting Information). The LUMO (a_2'' in idealized D_{3h}) is π* in character between the 3d$_{xz}$ orbitals on each copper center and the 3p$_z$ on sulfur and is calculated to be ~2 eV both above the HOMO and below the LUMO+1. The similar energies for the HOMO to HOMO-4 orbitals suggest that the broad nIR absorption could have contributions from ligand nonbonding to copper charge transfers as well as S(p) → Cu(3d). These transitions could account for the discrepancy between our UV−visible−nIR analysis and the electrochemical data regarding the extent of delocalization as well as the irreversible oxidative wave observed in the cyclic voltammogram of **3**. However, time-dependent DFT methods and other spectroscopic methods, such as magnetic circular dichroism, would be required to definitively assign the constituent transitions in this absorption band.

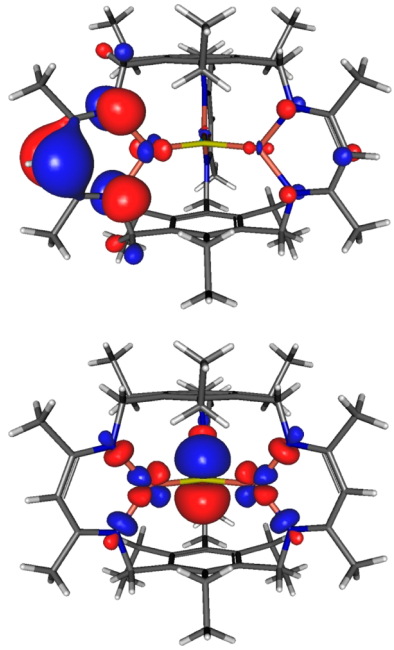

Figure 5. Calculated probability surfaces of the HOMO with pseudo e' symmetry (top) and LUMO with pseudo a_2'' symmetry (bottom) of **3** at an isovalue of 0.04. The HOMO is predominantly composed of the nonbonding π-type orbitals on the β-diketiminate arms, whereas the LUMO is S(3p$_z$)−Cu(3d$_{xz}$) π-antibonding.

Chemical Reduction of 3. Reduction of **3** with decamethylcobaltocene affords the turquoise-colored one-electron reduced complex, **4** (84% yield). ESI(-) mass spectra support retention of the cluster after reduction as the parent [Cu_3**SL**]$^-$ ion is observed (Figure S27, Supporting Information). The X-band EPR room-temperature spectrum of **4** is an isotropic ten-line absorption that corresponds to the SOMO being delocalized over the three $I = {}^3/_2$ Cu nuclei (Figure 6). For simplicity, we assumed three equivalent Cu atoms and omitted any hyperfine coupling from the N-atom donors in our Easy Spin[22] simulation of this room-temperature spectrum, which yields A and g values of 33 G and 2.095, respectively (Figure 5). Simulations of the 5 K spectrum using this simplified model were unsatisfactory, however, and will require

dx.doi.org/10.1021/ic500333p | Inorg. Chem. 2014, 53, 4647−4654

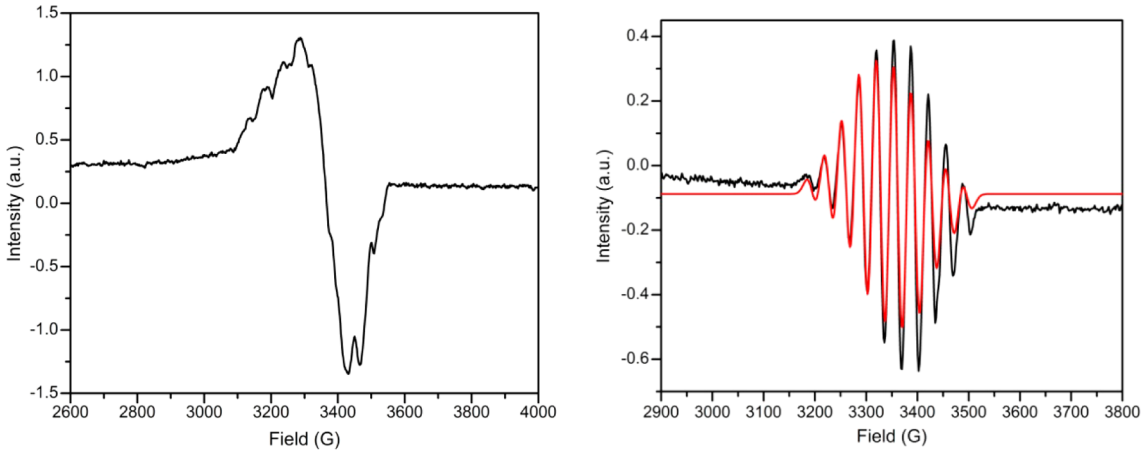

Figure 6. X-band EPR spectra of **4** in 2-methyltetrahydrofuran collected in perpendicular mode at 5 K (left) and 298 K (right). At room temperature, a ten-line absorption is observed (black line), which can be simulated with values of g = 2.095 and A = 33 G (red line), indicating delocalization of the unpaired electron over all three copper centers.

high-field experiments, which is beyond the scope of this report. These values are comparable to those reported by Tolman and co-workers for a self-assembled di(μ_3-sulfido)tricopper cluster as well as those for other copper−diketiminate complexes.[5,13a,16] In the electronic absorption spectrum of **4**, the nIR absorption band is blue-shifted (λ_{max} = 14 600 cm^{-1}) and narrower relative to **3** with calculated values for H_{ab} and Γ of 7300 cm^{-1} and 2.6, respectively (Figure 4). Taken together, the EPR spectra, the lower limit for the comproportionation constant (K_c > 3.02 × 10^{10}) as estimated from cyclic voltammetry, and the nIR data suggest that **4**, like **3**, is valence-delocalized and either a Class II or a Class III system.[20]

DISCUSSION

In the proposed structure of Cu_3**L**, **1**, we have tentatively assigned each cuprous ion as two-coordinate and bound in each nacnac arm, which has not been observed in Cu(nacnac) complexes to date. In all prior reports, each Cu(I) center is three coordinate with solvent bound to one site. Here, however, our speculative structure relies on NMR and elemental analysis for **1**. First, we analyzed the C, H, N, Cu, and Br contents of samples of **1**, and no bromide was observed within the detection limits of the instrumentation, which strongly indicates that a μ_3-bromide donor is not present in this complex. Second, NMR spectra confirm that D_{3h} symmetry is retained even at low temperature; thus, structures such as one in which each Cu^I center coordinates to the adjacent nacnac arm are inconsistent with these data. Such configurations would afford diastereotopic methylene protons for both the −C**H**$_2$CH$_3$ and −C**H**$_2$N, which we have been able to resolve in spectra with C_{3h}-symmetric main-group complexes of this ligand.[23] However, we cannot eliminate fluxional coordination of the copper centers between the N-donor site of the nacnac arms and the aromatic rings of the ligand, which has been observed in mononuclear complexes of monovalent late 3d-metal ions, or metal−metal interactions.[13b,24] Indeed, the absorption feature at ∼323 nm in **1** is of similar energy to those reported for other di- and trinuclear copper clusters and is typically the excitation band for the luminescence associated with these clusters.[25] Ongoing work is focused on exploring the photophysical properties of our tricuprous compounds to probe possible interactions between the metal centers. Drawing parallels between Cu_3**L** and the tricopper active sites of the multicopper oxidases, the steric constraints imposed by **L**$^{3-}$ are anticipated to enforce a coplanar orientation of O_2 relative to the tricopper plane, which is consistent with the proposed substrate binding mode in the enzyme system but remains uncommon in copper coordination complexes.[2]

Although the internal cavity in this ligand system can accommodate only one bridging atom, prior work clearly demonstrates that μ_2-donor atoms are readily accommodated within the space between two nacnac arms. We were, therefore, surprised by the selective formation of the (μ_3-sulfido)tricopper cluster because our results sharply contrast the disulfide- or di(μ_n-sulfide)-bridged compounds reported from reaction of N-donor copper(I) complexes with S atom sources.[5] We envisioned two possible mechanisms by which S_8 activation leads to **3**: by abstraction of a single S atom or by formation of a transient (μ_2-sulfido)(μ_3-sulfido)tricopper(II/III) cluster. In the latter case, the S···S vector would be sterically forced to lie parallel to the tricopper plane, which differs from previous reports in which the S···S vector is orthogonal to the plane of the three metal centers. Chan and co-workers reported a tricopper complex proposed to enforce a similar coplanar arrangement during O_2 activation, leading to a (μ_2-oxo)(μ_3-oxo)tricopper intermediate, which activates strong C−H bonds, and ultimately afford a mixed-valent oxo-bridged analogue of **3**.[26] To probe the possible intermediacy of a reactive di(μ-sulfide) or μ-disulfide complex, we reacted Cu_3**L** with S_8 in the presence of excess 9,10-dihydroanthracene, hydroquinone, or cyclohexene (data not shown). In all cases, however no products consistent with either C−H bond activation (viz. anthracene and *p*-quinone) or S atom transfer (viz. cyclohexene sulfide) are observed by GC/MS or ^{1}H NMR analysis of the reaction mixtures using benzene, toluene, or THF as the reaction solvent. In contrast, the sulfide-bridged complex is observed as a minor product with the protonated ligand as the predominant species in ^{1}H NMR spectra of reaction of Me_3PS with Cu_3**L** (Figure S24, Supporting Information). We speculate that the free ligand arises from complex decomposition in which the free phosphine generated upon reaction of R_3PS with **1** abstracts Cu^I from unreacted Cu_3**L** (Figure S25, Supporting Information). These data point to a mechanism for S_8 activation in this sterically constrained complex that is distinct from that for their self-assembled analogues.

dx.doi.org/10.1021/ic500333p | Inorg. Chem. 2014, 53, 4647−4654

From the electrochemical data and single-point calculations carried out on **3**, we assign the irreversible oxidation at 0.01 V in the cyclic voltammogram as a ligand-based event, which leads to complex decomposition. Similar noninnocence and facile oxidation of the nacnac nonbonding π-type orbitals have been observed in other β-diketiminate complexes.[27] In contrast, the reversible redox process at −1.44 V (vs Fc/Fc^+) would correlate to reduction of the cluster to generate the corresponding $[Cu_3S]^{2+}$ core. For the reduction of **3** by one electron to give **4**, the EPR spectrum clearly indicates that the SOMO is delocalized over all three copper centers. This result agrees with both our initial assignment of the reversible redox process at −1.44 V for **3** as cluster-based and also our DFT calculations in which the LUMO is also delocalized over the three metal atoms. Here, we simulated the data using a simplified model in which the copper centers were considered indistinguishable, and we are in the process of probing the charge delocalization in compound **4** by other methods.

CONCLUSION

In conclusion, we report the synthesis and characterization of a family of tricopper compounds, in which a cyclophane is used to preorganize and dictate the coordination environment of each metal center. In these complexes, each copper ion is coordinatively unsaturated, opening avenues to future studies on the reactivity of complexes **1**, **2**, and **4** with substrates, such as N_3^-, N_2O, and O_2. In addition, compounds **3** and **4** represent the first copper-containing clusters wherein each metal center is held in a N-rich coordination environment, coordinatively unsaturated, and bridged by an inorganic sulfide.

ASSOCIATED CONTENT

Supporting Information

Experimental details, supporting figures, computational methods, and X-ray crystallographic data in CIF format are available in the Supporting Information. This material is available free of charge via the Internet at http://pubs.acs.org.

AUTHOR INFORMATION

Corresponding Author

*E-mail: murray@chem.ufl.edu.

Author Contributions

The manuscript was written through contributions of all authors. All authors have given approval to the final version of the manuscript.

Funding

Research was supported by University of Florida, ACS Petroleum Research Fund (ACS-PRF 52704-DNI3), and instrumentation awards from the National Science Foundation (CHE-0821346 and CHE-1048604).

Notes

The authors declare no competing financial interest.

ACKNOWLEDGMENTS

The authors thank N. Roehr and Prof. N. C. Polfer for variable-temperature absorption data collection, U. Twahir and Prof. A. Angerhofer for assistance measuring EPR spectra, and Prof. M. Meisel and A. D. Mitchell for help with EPR simulations.

REFERENCES

(1) (a) Lieberman, R. L.; Rosenzweig, A. C. *Nature* **2005**, *434*, 177. (b) Hakemian, A. S.; Rosenzweig, A. C. *Annu. Rev. Biochem.* **2007**, *76*, 223. (c) Himes, R. A.; Barnese, K.; Karlin, K. D. *Angew. Chem., Int. Ed.* **2010**, *49*, 6714.

(2) (a) Solomon, E. I.; Sundaram, U. M.; Machonkin, T. E. *Chem. Rev.* **1996**, *96*, 2563. (b) Taylor, A. B.; Stoj, C. S.; Ziegler, L.; Kosman, D. J.; Hart, P. J. *Proc. Natl. Acad. Sci. U.S.A.* **2005**, *102*, 15459. (c) Solomon, E. I.; Augustine, A. J.; Yoon, J. *Dalton Trans.* **2008**, 3921. (d) Heppner, D. E.; Kjaergaard, C. H.; Solomon, E. I. *J. Am. Chem. Soc.* **2013**, *135*, 12212.

(3) (a) Rosenzweig, A. C. *Nat. Struct. Biol.* **2000**, *7*, 169. (b) Haltia, T.; Brown, K.; Tegoni, M.; Cambillau, C.; Saraste, M.; Mattila, K.; Djinovic-Carugo, K. *Biochem. J.* **2003**, *369*, 77. (c) Paraskevopoulos, K.; Antonyuk, S. V.; Sawers, R. G.; Eady, R. R.; Hasnain, S. S. *J. Mol. Biol.* **2006**, *362*, 55. (d) Pomowski, A.; Zumft, W. G.; Kroneck, P. M. H.; Einsle, O. *Nature* **2011**, *477*, 234. (e) Johnston, E. M.; Dell'Acqua, S.; Ramos, S.; Pauleta, S. R.; Moura, I.; Solomon, E. I. *J. Am. Chem. Soc.* **2014**, *136*, 614.

(4) (a) Cole, A. P.; Root, D. E.; Mukherjee, P.; Solomon, E. I.; Stack, T. D. P. *Science* **1996**, *273*, 1848. (b) Lionetti, D.; Day, M. W.; Agapie, T. *Chem. Sci.* **2013**, *4*, 785. (c) Gupta, A. K.; Tolman, W. B. *Inorg. Chem.* **2012**, *51*, 1881.

(5) (a) Brown, E. C.; York, J. T.; Antholine, W. E.; Ruiz, E.; Alvarez, S.; Tolman, W. B. *J. Am. Chem. Soc.* **2005**, *127*, 13752. (b) Brown, E. C.; Bar-Nahum, I.; York, J. T.; Aboelella, N. W.; Tolman, W. B. *Inorg. Chem.* **2007**, *46*, 486. (c) York, J. T.; Bar-Nahum, I.; Tolman, W. B. *Inorg. Chem.* **2007**, *46*, 8105. (d) York, J. T.; Bar-Nahum, I.; Tolman, W. B. *Inorg. Chim. Acta* **2008**, *361*, 885. (e) Bar-Nahum, I.; York, J. T.; Young, V. G., Jr.; Tolman, W. B. *Angew. Chem., Int. Ed.* **2008**, *47*, 533. (f) Inosako, M.; Kunishita, A.; Shimokawa, C.; Teraoka, J.; Kubo, M.; Ogura, T.; Sugimoto, H.; Itoh, S. *Dalton Trans.* **2008**, 6250. (g) Bar-Nahum, I.; Gupta, A. K.; Huber, S. M.; Ertem, M. Z.; Cramer, C. J.; Tolman, W. B. *J. Am. Chem. Soc.* **2009**, *131*, 2812.

(6) Armarego, W. L. F.; Chai, C. L. L. *Purification of Laboratory Chemicals*, 6th ed.; Elsevier: 2009.

(7) Bartlett, P. D.; Cox, E. F.; Davis, R. E. *J. Am. Chem. Soc.* **1961**, *83*, 103.

(8) Szczepanski, J.; Roser, D.; Personette, W.; Eyring, M.; Pellow, R.; Vala, M. *J. Phys. Chem.* **1992**, *96*, 7876.

(9) Guillet, G. L.; Sloane, F. T.; Ermert, D. M.; Calkins, M. W.; Peprah, M. K.; Knowles, E. S.; Čižmár, E.; Abboud, K. A.; Meisel, M. W.; Murray, L. J. *Chem. Commun.* **2013**, *49*, 6635.

(10) Frisch, M. J.; Trucks, G. W.; Schlegel, H. B.; Scuseria, G. E.; Robb, M. A.; Cheeseman, J. R.; Scalmani, G.; Barone, V.; Mennucci, B.; Petersson, G. A.; Nakatsuji, H.; Caricato, M.; Li, X.; Hratchian, H. P.; Izmaylov, A. F.; Bloino, J.; Zheng, G.; Sonnenberg, J. L.; Hada, M.; Ehara, M.; Toyota, K.; Fukuda, R.; Hasegawa, J.; Ishida, M.; Nakajima, T.; Honda, Y.; Kitao, O.; Nakai, H.; Vreven, T.; Montgomery, J. A., Jr.; Peralta, J. E.; Ogliaro, F.; Bearpark, M.; Heyd, J. J.; Brothers, E.; Kudin, K. N.; Staroverov, V. N.; Kobayashi, R.; Normand, J.; Raghavachari, K.; Rendell, A.; Burant, J. C.; Iyengar, S. S.; Tomasi, J.; Cossi, M.; Rega, N.; Millam, N. J.; Klene, M.; Knox, J. E.; Cross, J. B.; Bakken, V.; Adamo, C.; Jaramillo, J.; Gomperts, R.; Stratmann, R. E.; Yazyev, O.; Austin, A. J.; Cammi, R.; Pomelli, C.; Ochterski, J. W.; Martin, R. L.; Morokuma, K.; Zakrzewski, V. G.; Voth, G. A.; Salvador, P.; Dannenberg, J. J.; Dapprich, S.; Daniels, A. D.; Farkas, Ö.; Foresman, J. B.; Ortiz, J. V.; Cioslowski, J.; Fox, D. J. *Gaussian 09*, Revision D.01; Gaussian, Inc.: Wallingford, CT, 2009.

(11) Bailey, P. J.; Coxall, R. A.; Dick, C. M.; Fabre, S.; Henderson, L. C.; Herber, C.; Liddle, S. T.; Loroño-González, D.; Parkin, A.; Parsons, S. *Chem.—Eur. J.* **2003**, *9*, 4820.

(12) Spencer, D. J. E.; Aboelella, N. W.; Reynolds, A. M.; Holland, P. L.; Tolman, W. B. *J. Am. Chem. Soc.* **2002**, *124*, 2108.

(13) (a) Spencer, D. J. E.; Reynolds, A. M.; Holland, P. L.; Jazdzewski, B. A.; Duboc-Toia, C.; Le Pape, L.; Yokota, S.; Tachi, Y.; Itoh, S.; Tolman, W. B. *Inorg. Chem.* **2002**, *41*, 6307. (b) Amisial, L. D.; Dai, X.; Kinney, R. A.; Krishnaswamy, A.; Warren, T. H. *Inorg. Chem.* **2004**, *43*, 6537.

(14) (a) Barrett, A. G. M.; Crimmin, M. R.; Hill, M. S.; Hitchcock, P. B.; Kociok-Köhn, G.; Procopiou, P. A. *Inorg. Chem.* **2008**, *47*, 7366. (b) Horn, B.; Limberg, C.; Herwig, C.; Feist, M.; Mebs, S. *Chem.*

Commun. **2012**, *48*, 8243. (c) Thirumoorthi, R.; Chiver, T. *Eur. J. Inorg. Chem.* **2012**, 3061. (d) Appelt, C.; Slootweg, J. C.; Lammertsma, K.; Uhl, W. *Angew. Chem., Int. Ed.* **2012**, *51*, 5911.
(15) Haynes, W. M., Ed. *CRC Handbook of Chemistry and Physics*, 94th ed.; CRC Press: Boca Raton, FL, 2013.
(16) (a) Holland, P. L.; Tolman, W. B. *J. Am. Chem. Soc.* **1999**, *121*, 7270. (b) Jazdzewski, B. A.; Holland, P. L.; Pink, M.; Young, V. G., Jr.; Spencer, D. J. E.; Tolman, W. B. *Inorg. Chem.* **2001**, *40*, 6097.
(17) (a) Coe, B. J.; Harris, J. A.; Hall, J. J.; Brunschwig, B. S.; Hung, S.-T.; Libaers, W.; Clays, K.; Coles, S. J.; Horton, P. N.; Light, M. E.; Hursthouse, M. B.; Garín, J.; Orduna, J. *Chem. Mater.* **2006**, *18*, 5907. (b) Basu, S.; Coskun, A.; Friedman, D. C.; Olson, M. A.; Benítez, D.; Tkatchouk, E.; Barin, G.; Yang, J.; Fahrenbach, A. C.; Goddard, W. A., III; Stoddart, J. F. *Chem.—Eur. J.* **2011**, *17*, 2107.
(18) Richardson, D. E.; Taube, H. *Coord. Chem. Rev.* **1984**, *60*, 107.
(19) (a) Mezei, G.; McGrady, J. E.; Raptis, R. G. *Inorg. Chem.* **2005**, *44*, 7271. (b) Rivera-Carrillo, M.; Chakraborty, I.; Mezei, G.; Webster, R. D.; Raptis, R. G. *Inorg. Chem.* **2008**, *47*, 7644.
(20) D'Alessandro, D. M.; Keene, F. R. *Chem. Soc. Rev.* **2006**, *35*, 424.
(21) (a) Alvarez, M. L.; Ai, J.; Zumft, W.; Sanders-Loehr, J.; Dooley, D. M. *J. Am. Chem. Soc.* **2000**, *123*, 576. (b) Rasmussen, T.; Berks, B. C.; Sanders-Loehr, J.; Dooley, D. M.; Zumft, W. G.; Thomson, A. J. *Biochemistry* **2000**, *39*, 12753. (c) Chen, P.; Cabrito, I.; Moura, J. J. G.; Moura, I.; Solomon, E. I. *J. Am. Chem. Soc.* **2002**, *124*, 10497.
(22) Stoll, S.; Schweiger, A. *J. Magn. Reson.* **2006**, *178*, 42.
(23) Ermert, D. M.; Gordon, J. B.; Abboud, K. A.; Murray, L. J. Unpublished results.
(24) (a) Dugan, T. R.; Sun, X.; Rybak-Akimova, E. V.; Olatunji-Ojo, O.; Cundari, T. R.; Holland, P. L. *J. Am. Chem. Soc.* **2011**, *133*, 12418. (b) Cowley, R. E.; Holland, P. L. *Inorg. Chem.* **2012**, *51*, 8352. (c) Lee, Y.; Sloane, F. T.; Murray, L. J. Unpublished results.
(25) (a) Dias, H. V. R.; Diyabalanage, H. V. K.; Rawashdeh-Omary, M. A.; Franzman, M. A.; Omary, M. A. *J. Am. Chem. Soc.* **2003**, *125*, 12072. (b) Fu, W.-F.; Gan, X.; Che, C.-M.; Cao, Q.-Y.; Zhou, Z.-Y.; Zhu, N. N.-Y. *Chem.—Eur. J.* **2004**, *10*, 2228. (c) Dias, H. V. R.; Diyabalanage, H. V. K.; Eldabaja, M. G.; Elbjeirami, O.; Rawashdeh-Omary, M. A.; Omary, M. A. *J. Am. Chem. Soc.* **2005**, *127*, 7489. (d) Omary, M. A.; Rawashdeh-Omary, M. A.; Gonser, M. W. A.; Elbjeirami, O.; Grimes, T.; Cundari, T. R. *Inorg. Chem.* **2005**, *44*, 8200.
(26) (a) Maji, S.; Lee, J. C.-M.; Lu, Y.-J.; Chen, C.-L.; Hung, M.-C.; Chen, P. P.-Y.; Yu, S. S.-F.; Chan, S. I. *Chem.—Eur. J.* **2012**, *18*, 3955. (b) Chan, S. I.; Lu, Y.-J.; Nagababu, P.; Maji, S.; Hung, M.-C.; Lee, M. M.; Hsu, I.-J.; Minh, P. D.; Lai, J. C.-H.; Ng, K. Y.; Ramalingam, S.; Yu, S. S.-F.; Chan, M. K. *Angew. Chem., Int. Ed.* **2013**, *52*, 3731.
(27) (a) Khusniyarov, M. M.; Bill, E.; Weyhermüller, T.; Bothe, E.; Wieghardt, K. *Angew. Chem., Int. Ed.* **2011**, *50*, 1652. (b) Marshak, M. P.; Chambers, M. B.; Nocera, D. G. *Inorg. Chem.* **2012**, *51*, 11190.
(28) Van der Sluis, P.; Spek, A. L. *Acta Crystallogr. A* **1990**, *A46*, 194.
(29) Sheldrick, G. M. *SHELXTL-Plus Structure Determination Software Programs*, Version 6.14; Bruker Analytical X-ray Instruments Inc.: Madison, WI, 1998.